Transport Parameter Estimations of Plasma Transport Dynamics Using the Extended Kalman Filter

Chao Xu, Yongsheng Ou, and Eugenio Schuster

***Abstract*—The accuracy of first-principle predictive models for the evolution of plasma profiles is sometimes limited by the lack of understanding of the plasma transport phenomena. It is possible then to develop approximate transport models for the prediction of plasma dynamics, which are consistent with the available diagnostic data. This data-driven approach, usually referred to as phenomenological modeling, arises as an alternative to the more classical theory-driven approach. In this paper, we propose a stochastic filtering approach based on an extended Kalman filter to provide real-time estimates of poorly known or totally unknown transport coefficients. We first assume that plasma dynamics is governed by tractable models obtained by first principles. However, the transport parameters are considered unknown and to be estimated. These estimates will be based solely on input/output diagnostic data and limited understanding of the transport physics. Numerical methods (e.g., finite differences) can be used to discretize the partial differential equation models both in space and time to obtain finite-dimensional discrete-time state-space representations. The system states and to-be-estimated parameters are then combined into an augmented state vector. The resulting nonlinear state-space model is used for the design of an extended Kalman filter that provides real-time estimations not only of the system states but also of the unknown transport coefficients. Simulation results demonstrate the effectiveness of the proposed method for a benchmark transport model in cylindrical coordinates.**

***Index Terms*—Extended Kalman filter, parameter estimations, plasma transport.**

I. Introduction

MATHEMATICAL modeling of plasma transport phenomena with modest complexity but capturing dominant dynamics is critical for plasma control design. Transport theories (classical, neoclassical, and anomalous) produce, under necessary assumptions, strongly nonlinear models based on partial differential equations (PDEs). However, the complexity of these models often makes them not useful for control design since it is very challenging, if not impossible, to synthesize compact and reliable control strategies based on these complicated mathematical models. As an alternative, data-driven modeling techniques, including system identification [1] and data assimilations [2], have the potential to obtain practical low-complexity dynamic models for the control of plasma systems.

Manuscript received July 13, 2009; revised November 18, 2009. First published January 19, 2010; current version published March 10, 2010. This work was supported by the NSF CAREER Award Program (ECCS-0645086).

The authors are with the Department of Mechanical Engineering and Mechanics, Lehigh University, Bethlehem, PA 18015 USA (e-mail: chx205@lehigh.edu; yoo205@lehigh.edu; schuster@Lehigh.edu).

Color versions of one or more of the figures in this paper are available online at http://ieeexplore.ieee.org.

Digital Object Identifier 10.1109/TPS.2009.2038220

Data-driven modeling techniques have been successfully used in the past to model plasma transport dynamics for active control design in nuclear fusion reactors (see, e.g., [3]–[6]). System identification using input/output (I/O) diagnostic data has been used to model the current profile dynamics in ASDEX Upgrade [4]. In the JET tokamak [6], a two-time-scale linear system is used to describe the dynamics of the magnetic and kinetic profiles around certain quasi-steady-state trajectories, where system matrices can be identified from the experimental or simulation data using system identification algorithms in [1]. In the L-mode discharges of the JT-60U tokamak [5], diffusive and nondiffusive coefficients of the momentum transport equation of the toroidal rotation profile dynamics are estimated from transient data obtained by modulating the momentum source.

First-principle modeling of the plasma profile dynamics usually results in multiple-input–multiple-output infinite-dimensional transport models. By using the method of averaging over magnetic surfaces, the transport model can be formulated into 1-D PDEs with respect to a variable indexing the magnetic surfaces [7], [8]. System identification, however, often generates dynamic models fitting the I/O diagnostic data but does not take into account the physical structure of the transport model obtained by first principles. In this case, the states of the identified models do not necessarily represent physical variables. In this paper, we propose instead to use the tractable 1-D PDE structure [8] of the first-principle model to estimate its transport coefficients using experimental data. Previous work following a similar approach includes [3, pp. 424–445], where Wang formulates a parameter identification problem for the electron transport model of a tokamak plasma governed by nonlinear PDEs and proposes a PDE-constrained optimization method to solve the parameter estimation problem.

Various numerical methods (such as the finite-difference method [9]) can be used to obtain fully spatial–temporal discretized models in terms of given spatial nodes and sampling rates. For finite-dimensional discrete-time systems, stochastic filters (e.g., the Kalman filter) can be used to estimate the system states based on the I/O measurements. In order to be able to also estimate system parameters, such as the transport coefficients, it is possible to define an augmented state vector which includes both the original system states and those to-be-estimated parameters. The overall discrete-time model becomes nonlinear, but stochastic filters (e.g., the extended Kalman filter) can still be used to estimate the augmented state vector.

This paper is organized as follows. We introduce a linear parabolic PDE system in Section II that retains the general structure of plasma transport models under the circular cylindrical approximation. Then, an explicit numerical discretization

scheme [9] is derived based on the finite-difference method over a given spatial–temporal grid. In Section III, the propagation stability of the numerical scheme is discussed. In Section IV, we summarize the extended Kalman filter theory used in this paper for the estimation of both system states and transport parameters. In Section V, we test the performance of the proposed method in simulations. We close this paper by stating conclusions and potential research topics in Section VI.

II. Parabolic Plasma Transport System

We consider the following parabolic transport system [8], [10]:

$$\frac{\partial x(\xi,t)}{\partial t} = \frac{1}{\xi}\frac{\partial}{\partial \xi}\left[\xi \vartheta(\xi)\frac{\partial x(\xi,t)}{\partial \xi}\right] + S_{\rm IN}(\xi,t) \tag{1}$$

$$\frac{\partial x(0,t)}{\partial \xi} = 0 \quad \frac{\partial x(1,t)}{\partial \xi} = S_{\rm BC}(t) \quad x(\xi,t_{\rm I}) = x_0(\xi) \tag{2}$$

where $x(\xi,t)$ represents a general plasma profile with respect to the normalized spatial coordinate $\xi \in [0,1]$ and time $t \in [t_I, t_F]$. The parameter $\vartheta(\xi)$ is unknown and to be estimated based on observational data. Interior and boundary controls are denoted by $S_{\rm IN}(\xi,t)$ and $S_{\rm BC}(t)$, respectively. The initial distribution is denoted by $x_0(\xi)$. Two approaches can be considered to parameterize the unknown coefficient $\vartheta(\xi)$.

1) *Spatial discretization*: Given a spatial grid division, $0 = \xi_0 < \xi_1 < \cdots < \xi_i < \cdots < \xi_M = 1$, we can use the to-be-identified discrete values $\vartheta(\xi_i)$'s, $i = 0, 1, \ldots, M$, to approximate the spatially distributed coefficient $\vartheta(\xi_i)$ based on the "simple function approximation"11[11]

$$\vartheta(\xi) \approx \sum_{i=0}^{M-1} \vartheta(\xi_i)\mathbf{1}_{[\xi_i,\xi_{i+1})} \tag{3}$$

where $\mathbf{1}_{[\xi_i,\xi_{i+1})}$ is the simple function, which is defined as one on $[\xi_i, \xi_{i+1})$ and zero elsewhere.

2) *Subspace approximation*: Given a subspace $\Theta^s = \{v_1^s(\xi), v_2^s(\xi), \ldots, v_{l_s}^s(\xi)\}$, where $v_i^s(\xi)$'s, $i = 0, 1, \ldots, l_s$, are basis functions, we assume that the unknown spatially distributed coefficient can be expressed by $\vartheta(\xi) \approx \sum_{i=1}^{l_s} \vartheta_i^s v_i^s(\xi)$, where the constants ϑ_i^s's are the to-be-identified parameters.

In this section, we follow the first approach and derive a discrete representation of the continuous PDE system (1) and (2) using an explicit scheme over the following spatial–temporal grid division:

$$0 = \xi_0 < \xi_1 < \cdots < \xi_i < \cdots < \xi_M = 1 \tag{4}$$

$$t_0 = t_I < t_1 < \cdots < t_j < \cdots < t_N = t_F \tag{5}$$

where $\xi_i = ih$ and $t_j = t_0 + jT$. The profile function is then rewritten as $x_i^j = x(\xi_i, t_j)$. The boundary conditions are discretized using the Taylor series expansions to obtain

$$\frac{\partial x(\xi_0,t_j)}{\partial \xi} = \frac{-3x_0^j + 4x_1^j - x_2^j}{2h} = 0 \tag{6}$$

$$\frac{\partial x(\xi_M,t_j)}{\partial \xi} = \frac{x_{M-2}^j - 4x_{M-1}^j + 3x_M^j}{2h} = S_{\rm BC}^j. \tag{7}$$

Over the interior nodes $\xi_1, \ldots, \xi_{M-1}$, we obtain the following discrete scheme:

$$\begin{aligned}\frac{x_i^{j+1} - x_i^j}{T} &= \vartheta_i \frac{x_{i-1}^j - 2x_i^j + x_{i+1}^j}{h^2} + \vartheta_i \frac{x_{i+1}^j - x_{i-1}^j}{2ih^2} + S_{{\rm IN},i}^j \\ &= \frac{\vartheta_i}{h^2}\left[\frac{2i-1}{2i}x_{i-1}^j - 2x_i^j + \frac{2i+1}{2i}x_{i+1}^j\right] + S_{{\rm IN},i}^j\end{aligned} \tag{8}$$

where we have used the simple function approximation (3) for the coefficient $\vartheta(\xi)$ and denoted $\vartheta_i = \vartheta(\xi_i)$. We substitute (6) and (7) into (8) for $i = 1$ and $i = M-1$, respectively. Then, we obtain the following discrete system:

$$\begin{cases} x_1^{j+1} = -\frac{4T\vartheta_1}{3h^2}\left[x_1^j - x_2^j\right] + x_1^j + TS_{{\rm IN},1}^j \\ x_i^{j+1} = \frac{T\vartheta_i}{h^2}\left[\frac{2i-1}{2i}x_{i-1}^j - 2x_i^j + \frac{2i+1}{2i}x_{i+1}^j\right] + x_i^j + TS_{{\rm IN},i}^j \\ x_{M-1}^{j+1} = \frac{2(M-2)T\vartheta_{M-1}}{3(M-1)h^2}x_{M-2}^j - \frac{2(M-2)T\vartheta_{M-1}}{3(M-1)h^2}x_{M-1}^j \\ \qquad + x_{M-1}^j + \frac{(2M-1)T\vartheta_{M-1}}{3(M-1)h}S_{\rm BC}^j + TS_{{\rm IN},M-1}^j. \end{cases} \tag{9}$$

Although our goal in this paper is to work with a general transport equation (1), to better illustrate the proposed estimation technique, a particular system output is adopted as

$$y(\xi,t) = \frac{1}{\xi}\frac{\partial x(\xi,t)}{\partial \xi}. \tag{10}$$

Note that if the state x in (1) represents the poloidal magnetic flux, the output defined y in (10) is related to the rotational transform [8], [6]. The proposed estimation method can indeed handle any arbitrary nonlinear function of the state for the system output. The output (10) can be discretized as

$$\begin{aligned} y_1^{j+1} &= \frac{1}{2h^2}\left[x_2^{j+1} - x_0^{j+1}\right] = \frac{2}{3h^2}\left[x_2^{j+1} - x_1^{j+1}\right] \\ y_i^{j+1} &= \frac{1}{2ih^2}\left[x_{i+1}^{j+1} - x_{i-1}^{j+1}\right], \qquad i = 2, \ldots, M-2 \\ y_{M-1}^{j+1} &= \frac{1}{\xi_{M-1}}\frac{\partial x(\xi_{M-1},t_{j+1})}{\partial \xi} = \frac{1}{(M-1)h}\frac{x_M^{j+1} - x_{M-2}^{j+1}}{2h} \\ &= \frac{2}{3(M-1)h^2}\left[x_{M-1}^{j+1} - x_{M-2}^{j+1}\right] + \frac{S_{\rm BC}^{j+1}}{3(M-1)h} \end{aligned} \tag{11}$$

where we have used the discretized boundary conditions (6) and (7) to replace x_0^{j+1} and x_M^{j+1} in the first and third equations of (11), respectively. Measurements of the system output are taken only at some discrete points in space, i.e., y_i, $i = 1, \ldots, M-1$.

Remark 1—System With Time-Varying Coefficient: When the transport coefficients are time varying, it is possible to follow a subspace approximation approach. We assume

that the time-varying functions can be approximated by certain temporal basis functions $v_i^t(t),\ i=0,1,\ldots,l_t$, spanning the subspace $\Theta^t=\{v_1^t(t),v_2^t(t),\ldots,v_{l_t}^t(t)\}$, i.e., $\vartheta(t)\approx\sum_{i=1}^{l_t}\vartheta_i^t v_i^t(t)$, where the constants ϑ_i^t's are the to-be-identified parameters.

III. Propagation Stability

We discuss now the stability of the discretized model with respect to the iteration index j, which is critical for effective estimation. This discussion is timely because textbooks (e.g., [12]) on stability of finite-difference schemes usually do not include boundary conditions in the analysis. In addition, the cylindrical geometry considered in this paper makes the stability analysis more complicated than in Euclidean coordinates usually found in textbooks. The propagation matrix of the discrete scheme (9) is denoted by $\Phi=A(\omega_1,\ldots,\omega_{M-1})+I$, where $\omega_i=T\vartheta_i/h^2\ \ (i=1,2,\ldots,M-1)$, I is an identity matrix, and A is the coefficient matrix of the discretization of the spatial derivatives in (9). By introducing a vector $\mathbf{x}^j$ as the collection of the unknowns $x_1^j,\ldots,x_{M-1}^j$, we can rewrite the discrete scheme (9) as

$$\mathbf{x}^{j+1}=\Phi\mathbf{x}^j+S^j \tag{12}$$

where S^j represents the source terms. Based on stability theory of linear systems [12], the numerical scheme is numerically stable if and only if all the eigenvalues of the propagation matrix Φ satisfy $|\lambda|<1$, where $\lambda\in\mathbb{C}$ solves the characteristic polynomial equation $\det(\lambda I-\Phi)=0$.

The matrix $(\lambda I-\Phi)$ takes a tridiagonal form

$$\lambda I-\Phi=\begin{bmatrix}\alpha_1 & \gamma_1 & & & \\ \beta_2 & \alpha_2 & \gamma_2 & & \\ & \cdots & \cdots & \cdots & \\ & & & \beta_{M-1} & \alpha_{M-1}\end{bmatrix}$$

where the parameters α's, β's, and γ's are functions of λ and ω_i, $i=0,1,\ldots,M-1$. We carry out an LU decomposition, $\lambda I-\Phi=LU$, with L and U defined by

$$L=\begin{bmatrix}l_1 & & & \\ \beta_2 & l_2 & & \\ & \cdots & & \\ & & \beta_{M-1} & l_{M-1}\end{bmatrix}\qquad U=\begin{bmatrix}1 & \mu_1 & & \\ & 1 & \mu_2 & \\ & & \cdots & \\ & & & 1\end{bmatrix}$$

where $l_1=\alpha_1$, $\mu_i=\gamma_i/l_i\ (i=1,\ldots,M-2)$, and $l_i=\alpha_i-\beta_i\mu_{i-1}\ \ (i=2,\ldots,M-1)$. Therefore, the λ-polynomial is determined by

$$p_{M-1}(\lambda,\omega)=\det(\lambda I-\Phi)=\det L=\Pi_{i=1}^{M-1}l_i \tag{13}$$

where ω denotes the collection of ω_i, $i=0,1,\ldots,M-1$.

For a general M, it is difficult to obtain the polynomial (13) manually, and a recursive approach is necessary. By rewriting

$$l_i=\alpha_i-\beta_i\gamma_{i-1}\Pi_{k=1}^{i-2}l_k/\Pi_{k=1}^{i-1}l_k,\qquad i=3,4,\ldots \tag{14}$$

we can calculate the polynomial (13) recursively as

$$p_1(\lambda,\omega)=l_1=\alpha_1 \tag{15}$$

$$p_2(\lambda,\omega)=l_1l_2=\alpha_1\alpha_2-\beta_2\gamma_1 \tag{16}$$

$$\begin{aligned}p_i(\lambda,\omega)&=\Pi_{k=1}^{i}l_k\\&=\alpha_i p_{i-1}-\beta_i\gamma_{i-1}p_{i-2},\qquad i\geq 3.\end{aligned} \tag{17}$$

As a special case, we calculate the polynomial (13) when $M=5$

$$\begin{aligned}p_4(\lambda,\omega)=\alpha_4\alpha_3\alpha_2\alpha_1-\alpha_4\alpha_3\beta_2\gamma_1\\-\alpha_4\beta_3\gamma_2\alpha_1-\beta_3\gamma_2\alpha_2\alpha_1+\beta_3\gamma_3\beta_2\gamma_1.\end{aligned} \tag{18}$$

We assume that the characteristic polynomial (13) can be represented by

$$p_{M-1}(\lambda)=\nu_0\lambda^{M-1}+\nu_1\lambda^{M-2}+\cdots+\nu_{M-2}\lambda+\nu_{M-1} \tag{19}$$

where the coefficients ν_i's, $i=0,1,\ldots,M-1$, depend on the discretization parameter $\omega_i=T\vartheta_i/h^2\ \ (i=1,2,\ldots,M-1)$ and are obtained through the recursive computations (15)–(17). By using the Routh–Hurwitz or Jury stability criteria [12], we can obtain a stability condition for the proposed explicit discretization scheme without the need of computing the roots of (19). This stability condition is expressed in terms of the parameters ω_i's, which are, in turn, functions of the coefficients ϑ_i's. Given ranges for ϑ_i, it is always possible to choose a time step T that is small enough to satisfy this stability condition. However, since the coefficients ϑ_i's are the to-be-estimated unknowns, their possible ranges are not well known *a priori*, which usually demands a conservative choice for the time step T.

IV. Extended Kalman Filter

We can define $\mathbf{u}^j=[\,S_{\mathrm{IN},i}^j\quad S_{\mathrm{BC}}^j\,]^{\mathrm{T}}$. By introducing the augmented state and system output

$$\mathbf{z}^j=[\,x_1^j\quad x_2^j\quad\cdots\quad x_{M-1}^j\quad\vartheta^j\,]^{\mathrm{T}} \tag{20}$$

$$\mathbf{y}^j=[\,y_1^j\quad y_2^j\quad\cdots\quad y_{M-1}^j\,]^{\mathrm{T}} \tag{21}$$

we can rewrite the discretized system (9)–(11) as the following nonlinear state space representation:

$$\mathbf{z}^{j+1}=f(\mathbf{z}^j,\mathbf{u}^j)+\mathbf{w}^j\qquad\mathbf{y}^{j+1}=h(\mathbf{z}^{j+1},\mathbf{u}^j)+\mathbf{v}^{j+1}$$

where f and h are the state and measurement mappings defined by the finite-difference schemes in (9)–(11) and the equation(s) for ϑ given by $\vartheta^{j+1}=\vartheta^j$. The disturbance input $\mathbf{w}$ and the measurement noise $\mathbf{v}$ are assumed to be white zero-mean Gaussian random sequences, i.e., $\mathbf{w}^j\sim N(0,Q^j)$ and $\mathbf{v}^j\sim N(0,R^j)$, which satisfy the following properties:

$$E[\mathbf{w}^{j_1}\cdot\mathbf{v}^{j_2}]=0\qquad\forall\, j_1,j_2 \tag{22}$$

$$E[\mathbf{v}^{j_1}\cdot\mathbf{v}^{j_2}]=0\quad E[\mathbf{w}^{j_1}\cdot\mathbf{w}^{j_2}]=0\qquad\forall j_1\neq j_2 \tag{23}$$

$$E[\mathbf{w}^j\cdot\mathbf{w}^j]=Q^j\quad E[\mathbf{v}^j\cdot\mathbf{v}^j]=R^j \tag{24}$$

where Q^j and R^j are covariance matrices.

In the rest of this section, we give a brief introduction of the extended Kalman filter which is the nonlinear version of the well-known Kalman filter in estimation theory. In the following equations, we use $\hat{\mathbf{z}}^{j+1|j}$ to represent the state propagation before the measurements are considered:

$$\hat{\mathbf{z}}^{j+1|j} = f(\hat{\mathbf{z}}^{j|j}, \mathbf{u}^j) \tag{25}$$

where $\hat{}$ represents the estimated value. We then compute the Jacobian matrices with respect to the current state $\hat{\mathbf{z}}^{j|j}$, the propagation state $\hat{\mathbf{z}}^{j+1|j}$, and the control input $\mathbf{u}^j$

$$F^j = \left.\frac{\partial f(\mathbf{z},\mathbf{u})}{\partial \mathbf{z}}\right|_{\hat{\mathbf{z}}^{j|j},\mathbf{u}^j} \qquad H^{j+1} = \left.\frac{\partial h(\mathbf{z},\mathbf{u})}{\partial \mathbf{z}}\right|_{\hat{\mathbf{z}}^{j+1|j},\mathbf{u}^j}. \tag{26}$$

We are able to improve the propagation result in (25) by taking into account the measurement $\mathbf{y}^{j+1}$

$$\hat{\mathbf{z}}^{j+1|j+1} = \hat{\mathbf{z}}^{j+1|j} + K^{j+1}\left[\mathbf{y}^{j+1} - h(\mathbf{z}^{j+1|j}, \mathbf{u}^j)\right] \tag{27}$$

where the gain K^{j+1} is determined as

$$\begin{aligned} P^{j+1|j} &= F^j P^{j|j} (F^j)^{\mathrm{T}} + Q^j \\ K^{j+1} &= P^{j+1|j}(H^{j+1})^{\mathrm{T}}\left[H^{j+1}P^{j+1|j}(H^{j+1})^{\mathrm{T}} + R^{j+1}\right]^{-1} \\ P^{j+1|j+1} &= (I - K^{j+1}H^{j+1})P^{j+1|j}. \end{aligned}$$

More details on the extended Kalman filter can be found in [2].

V. Numerical Example

A. Numerical Simulation of the PDE System—Dense Grid

We first solve the PDE system (1) and (2) on a dense grid based on an implicit finite-difference scheme. The interior actuation function is assumed of the form $S_{\mathrm{IN}}(\xi,t) = b_{\mathrm{in}}(\xi)S^*_{\mathrm{IN}}(t)$, which is indeed a relatively good model approximation for present spatially distributed actuators (e.g., current drives, torque sources, pellet injectors, etc.). We assume the deposition profile as $b_{\mathrm{in}}(\xi) = 1 - \xi^4$ $(0 \le \xi \le 1)$ and the excitation signals (shown in Fig. 1) as

$$S^*_{\mathrm{IN}}(t) = \frac{1}{3}\sin(5t) + \frac{1}{2}\cos\left[10t + \cos(5t^2)\right] \tag{28}$$

$$S_{\mathrm{BC}}(t) = \frac{3}{2}\sin\left(\frac{1}{5}t^2\right). \tag{29}$$

The deposition profile and excitation signals have been arbitrarily chosen to illustrate the method through a simulation study. In practice, we are always interested in exciting the system in a broad range of frequencies. These types of excitation signals can indeed be implemented in real experiments.

The spatial–temporal domain is given by $\Omega = \{(\xi,t) : 0 \le \xi \le 1, 0 \le t \le 6\}$. To start the simulation, the initial distribution is assumed as $x(\xi,0) = x_0(\xi) = 2 - (4/5)\xi^2$. The simulation of system (1) and (2) is carried out over the grid nodes (4) and (5) with time step $T = T_d = 0.05$ (s) and spatial step $h = h_d = 0.025$, where we use the subscript d to denote a dense-grid division. The spatial–temporal evolution obtained from the numerical simulation for the case $\vartheta = 0.12$ constant is shown in Fig. 2, where the evolutionary trajectories corresponding to the values at the four finite-difference node points used for the extended Kalman filter are marked with red solid lines on the 3-D surface.

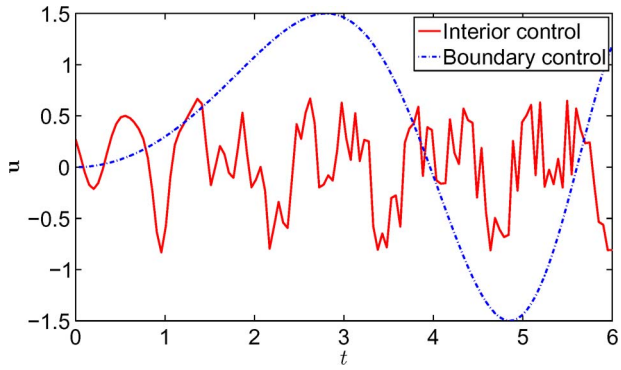

Fig. 1. (Red solid line) Interior and (blue dotted line) boundary excitation signals defined by (28) and (29).

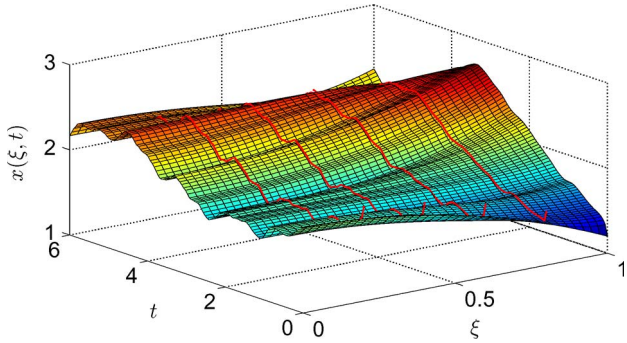

Fig. 2. Spatial–temporal evolution of the PDE system (1) and (2) with excitation signals (28) and (29).

B. Design of Extended Kalman Filter—Sparse Grid

We now let $h = h_s = 0.2$ and $T = T_s = 0.05$, where the subscript s denotes a sparse-grid division. We use an explicit difference scheme to obtain a fourth-order discrete system based on (9). The measurements defined by (10) are also taken at the same spatial nodes that are used to obtain the state propagation scheme (9).

Initial guesses for both the system states and transport parameters are needed to start the estimation. The better the guesses for the system states, the better and faster the estimation of the transport parameters. When the main goal is the estimation of the transport parameters, it is worth taking advantage of the fact that direct or indirect measurements of the states are usually available in present tokamaks either in real time or computed off-line from previous discharges. Therefore, in this simulation study, we assume that the initial guesses for the system states are indeed slightly perturbed versions of the real ones. For simulation purposes, we assume that the initial state distribution is given by $x(\xi,0) = x_0(\xi) = 2 - (4/5)\xi^2$. The numerical simulations discussed hereinafter use the same settings for the initial profile, discretization steps, and excitation signals defined earlier in this section. We first consider the case where the transport coefficient is constant and given by $\vartheta = 0.12$. The initial guess for the parameter is instead given by $\hat{\vartheta} = 0.23$. The initial guess error for the states is within

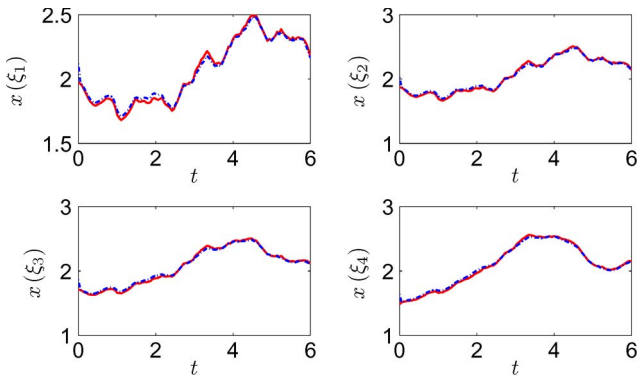

Fig. 3. (Red solid line) Actual and (blue dotted line) estimated states.

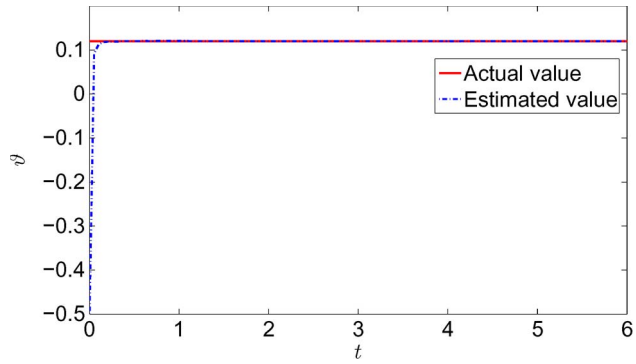

Fig. 4. (Red solid line) Actual and (blue dotted line) estimated coefficients.

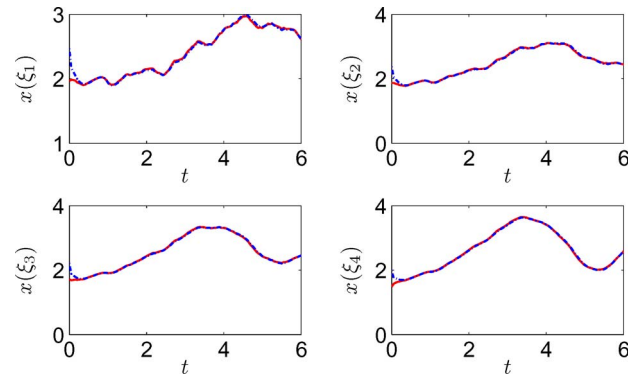

Fig. 5. (Red solid line) Actual and (blue dotted line) estimated states.

10% of the real value. With the given initial settings, we use the extended Kalman filter to obtain both state and parameter estimations, which are shown in Figs. 3 and 4, respectively. The parameter estimation can rapidly converge to the real value.

We now consider the case where the transport coefficient is spatially distributed. Instead of having only one unknown parameter, we use four values at different node points $\vartheta(\xi_i)$'s, $i = 1, 2, 3, 4$, to represent the transport coefficient $\vartheta(\xi)$. The actual distributed transport coefficient is given by $\vartheta(\xi) = 0.8\xi^2$. The initial guesses to start the parameter estimation are given by $(\hat{\vartheta}_1, \hat{\vartheta}_2, \hat{\vartheta}_3, \hat{\vartheta}_4) = (0.13, 0.23, 0.13, 0.33)$. The initial guess error for the states is within 25% of the real value. It is shown in Figs. 5 and 6 that the extended Kalman filter can effectively provide the estimations of both the system states and the transport coefficients.

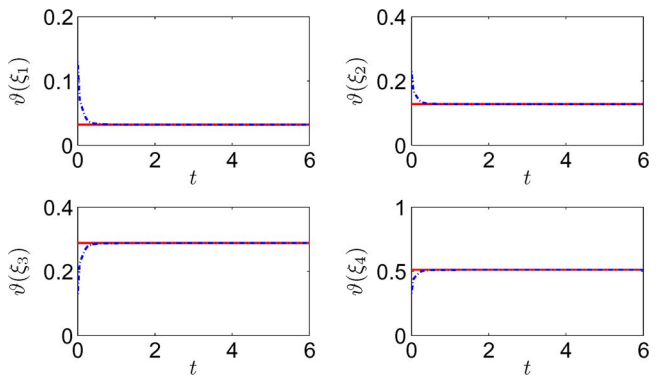

Fig. 6. (Red solid line) Actual and (blue dotted line) estimated coefficients.

VI. Conclusion

We have considered a parameter estimation problem for a benchmark model in plasma transport, which is governed by a 1-D parabolic PDE. The explicit scheme is then used to obtain a finite-dimensional discrete-time approximation based on the finite-difference discretization of the PDE system over a given spatial–temporal grid division. By including the unknown transport coefficient as an augmented state variable, we are able to reformulate the discrete-time linear system into an augmented nonlinear system. Then, the extended Kalman filtering technique is used to obtain real-time estimations of both the system state and the transport coefficient based on the measurements.

In this paper, we have only considered the case where the to-be-estimated parameter is independent of time. However, by parameterizing time-varying transport parameters via given temporal basis functions, it may be possible to formulate the estimation problems of temporally distributed parameters within the framework discussed in this paper. In this case, the objective would be to estimate the constant projections of the time-varying transport coefficients on the set of temporal basis functions.

In order to avoid reducing T excessively in order to satisfy the stability condition for the proposed explicit discretization scheme, implicit *unconditionally stable* discretization schemes must be developed as part of our future work to obtain robust parameter estimations. The achievement of this goal will require a modification of the extended Kalman filter since it is not well suited for the model structure resulting from the implicit discretization procedure.

This paper has presented an alternative to the first-principle approach to the modeling of the plasma dynamics and transport phenomena by assimilating the experimental observations into transport PDE models with modest complexity. Since the assimilation of experimental data is carried out in real time, this method can be effectively integrated into a feedback plasma control system.

References

[1] L. Ljung, *System Identification: Theory for the User*. Englewood Cliffs, NJ: Prentice-Hall PTR, 1999.

[2] B. Anderson and J. Moore, *Optimal Filtering*. Englewood Cliffs, NJ: Prentice-Hall, 1979.

[3] P. Wang, *Distributed Parameter Systems: Modelling and Identification*. Berlin, Germany: Springer-Verlag, 1978.
[4] Y.-S. Na, *Modelling of Current Profile Control in Tokamak Plasmas*. Munich, Germany: Fakultat fur Physik: Technische Universitat Munchen, 2003.
[5] M. Yoshida, Y. Koide, H. Takenaga, H. Urano, N. Oyama, K. Kamiya, Y. Sakamoto, G. Matsunaga, and Y. Kamada, "Momentum transport and plasma rotation profile in toroidal direction in JT-60U L-mode plasmas," *Nucl. Fus.*, vol. 47, no. 8, pp. 856–863, Aug. 2007.
[6] D. Moreau, D. Mazon, A. Ariola, G. De Tommasi, L. Laborde, F. Piccolo, F. Sartori, T. Tala, L. Zabeo, A. Boboc, E. Bouvier, M. Brix, J. Brzozowski, C. D. Challis, V. Cocilovo, V. Cordoliani, F. Crisanti, E. De La Luna, R. Felton, N. Hawkes, R. King, X. Litaudon, T. Loarer, J. Mailloux, M. Mayoral, I. Nunes, E. Surrey, and O. Zimmerman, "A two-time-scale dynamic-model approach for magnetic and kinetic profile control in advanced tokamak scenarios on JET," *Nucl. Fus.*, vol. 48, no. 10, p. 106 001, Oct. 2008.
[7] F. Hinton and R. Hazeltine, "Theory of plasma transport in toroidal confinement systems," *Rev. Mod. Phys.*, vol. 48, no. 2, pp. 239–308, Apr. 1976.
[8] J. Blum, *Numerical Simulation and Optimal Control in Plasma Physics*. New York: Wiley, 1989.
[9] J. Strikwerda, *Finite Difference Schemes and Partial Differential Equations*, 2nd ed. Philadelphia, PA: SIAM: Soc. Ind. Appl. Math., 2004.
[10] K. Gentle, "Dependence of heat pulse propagation on transport mechanisms: Consequences of nonconstant transport coefficients," *Phys. Fluids*, vol. 32, pp. 1241–1258, 1992.
[11] W. Rudin, *Real and Complex Analysis*. New York: Tata McGraw-Hill, 2006.
[12] P. Sarachik, *Principles of Linear Systems*. New York: Cambridge Univ. Press, 1997.

Chao Xu, photograph and biography not available at the time of publication.

Yongsheng Ou, photograph and biography not available at the time of publication.

Eugenio Schuster, photograph and biography not available at the time of publication.